Int. J. Electrochem. Sci., 8 **(2013)** 11951 - 11971

International Journal of
ELECTROCHEMICAL
SCIENCE
www.electrochemsci.org

Inhibition Effect of *N*-(2-chlorobenzylidene)-4-acetylaniline on the Corrosion of Stainless Steel

Mieczyslaw Scendo[*], *Joanna Trela*

Institute of Chemistry, Jan Kochanowski University in Kielce, ul. Swietokrzyska 15G, PL – 25406 Kielce, Poland
[*]E-mail: scendo@ujk.edu.pl

Received: 20 June 2013 / *Accepted:* 29 July 2013 / *Published:* 10 September 2013

The influence of the concentration of *N*-(2-chlorobenzylidene)-4-acetylaniline (CBAA) on the corrosion of 304 austenic stainless steel (ASS) in chloride acid solutions was studied. The potentiodynamic polarization, quantum chemical calculations and scanning electron microscopy (SEM) have been used. The inhibition efficiency increased with an increase in the concentration of CBAA. The polarization study revealed that CBAA acted as a mixed-type inhibitor. The adsorption of *N*-(2-chlorobenzylidene)-4-acetylaniline onto the ASS surface occur according to the Langmuir isotherm. The corrosion kinetic parameters of 304 austenic stainless steel, adsorption thermodynamic parameters, and quantum chemical parameters for CBAA were determined and discussed.

Keywords: A, Austenic stainless steel; A, *N*-(2-chlorobenzylidene)-4-acetylaniline; Potentiodynamic polarization; C, Corrosion inhibition; C, Kinetic parameters

1. INTRODUCTION

Conventional austenic stainless steel has a wide scope of applications in different industries. The corrosion resistance of all types of austenic stainless steel is based on the bilayer structure of the spontaneously formed passive films on their surface in aqueous solutions or in the contact with moist air [1]. Passive oxide films on stainless steel are usually very thin, consisting primarily of chromium oxide, Cr_2O_3 [2]. The barrier properties of passive films significantly decrease in the presence of chloride ions, which cause localized corrosion phenomena [3]. Corrosion inhibitors can be used to reduce the corrosion rate of metals exposed to corrosive environments. Schiff base compounds have been previously reported as corrosion inhibitors for copper, aluminum, and steel [4-10]. The Schiff base is an organic compound formed by the condensation of an amine and a carbonyl group having general formula of R_1 –CH = N– R_2 where R_1 and R_2 are aryl, alkyl, cycloalkyl or heterocyclic groups.

The primary advantages of many Schiff base compounds are that they can be conveniently and easily synthesized from relatively cheap materials and that they are eco-friendly or exhibit low toxicity [11]. Some research workers reveal that the inhibition efficiency of Schiff bases are much greater than the corresponding amines and ketone/aldehydes [12-14]. Several Schiff bases have recently been investigated as corrosion inhibitors for the mild and carbon steels in hydrochloric acid media [15-21]. These substances generally become effective due to the presence of an imine group. The adsorption on the metal surface can be attributed to coordination of the organic compounds via phenol and imines groups. Besides the imine group substitution of different groups also affects the inhibition properties. These compounds in general are adsorbed on the metal surface blocking the active corrosion sites. Inhibition efficiency of an inhibitor depends on the number of adsorption active centers in the molecule and their charge densities, the molecule size, and the mode of adsorption on the metal surface [22,23].

The aim of this study is the investigation of inhibition effect of *N*-(2-chlorobenzylidene)-4-acetylaniline (CBAA) (Schiff base) on the corrosion of 304 austenic stainless steel (ASS) in 1.2 M chloride solutions. Potentiodynamic polarization, quantum chemical calculations and scanning electron microscopy SEM) have been used. The best isotherm has been selected and the effect of the temperature (25 – 60 ^{0}C) on the corrosion behavior of austenic stainless steel in the absence and presence CBAA have been investigated.

2. EXPERIMENTAL

2.1. Solutions

The electrolytes were prepared using analytical grade NaCl and HCl reagents (Merck). The corrosive medium 1.2 M Cl^-, was prepared from a stock of NaCl and 1.0 M HCl solution. All solutions were prepared from double distilled water. The pH of all solutions was 1.5. For each experiment a freshly made solution was used. All tests were performed in naturally aerated electrolytes.

2.2. Materials

The testing material was austenitic stainless steel type 304. The steel composition was as follows (in wt.%): C: 0.079, Cr: 18.97, Ni: 10.78, Mn: 1.47, Mo: 0.56, Si: 0.61, P: 0.043, S: 0.05, N: 0.04 and Fe: balance.

Figure 1 shows a typical microstructure of the austenic stainless steel of the present study in the mill-annealed condition. Equiaxed grains free of precipitates and containing annealing twins were observed. The average grain size of the steels were nearly the same and varied in the range of 29 - 49 μm. The austenic 304 stainless steel was chosen for investigation regard on remarkably mechanical properties, high corrosion resistance in various aggressive environments, and common use in many civil constructions in marine or industrial environments [24].

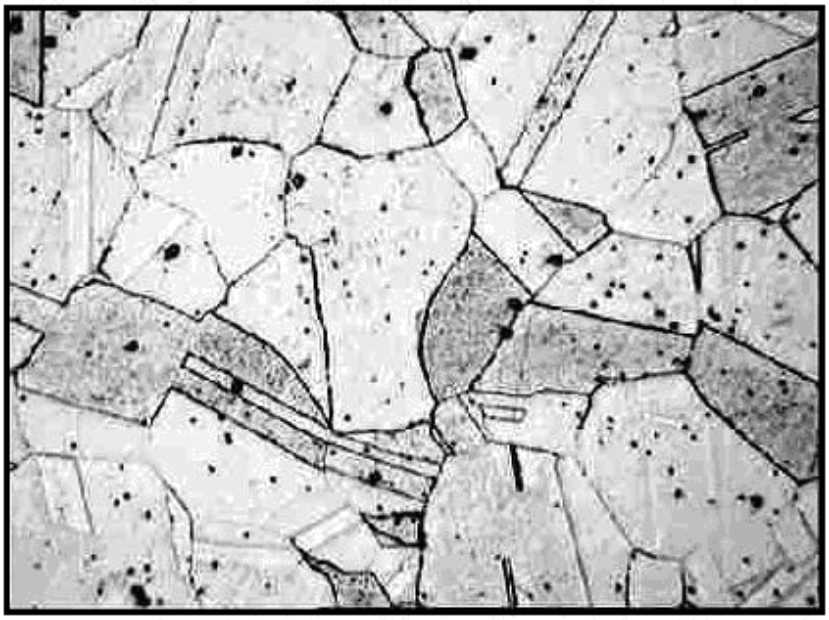

Figure 1. Microstructure of 304 austenic stainless steel

2.3. Inhibitor

The structure of *N*-(2-chlorobenzylidene)-4-acetylaniline (CBAA) is given in Figure 2.

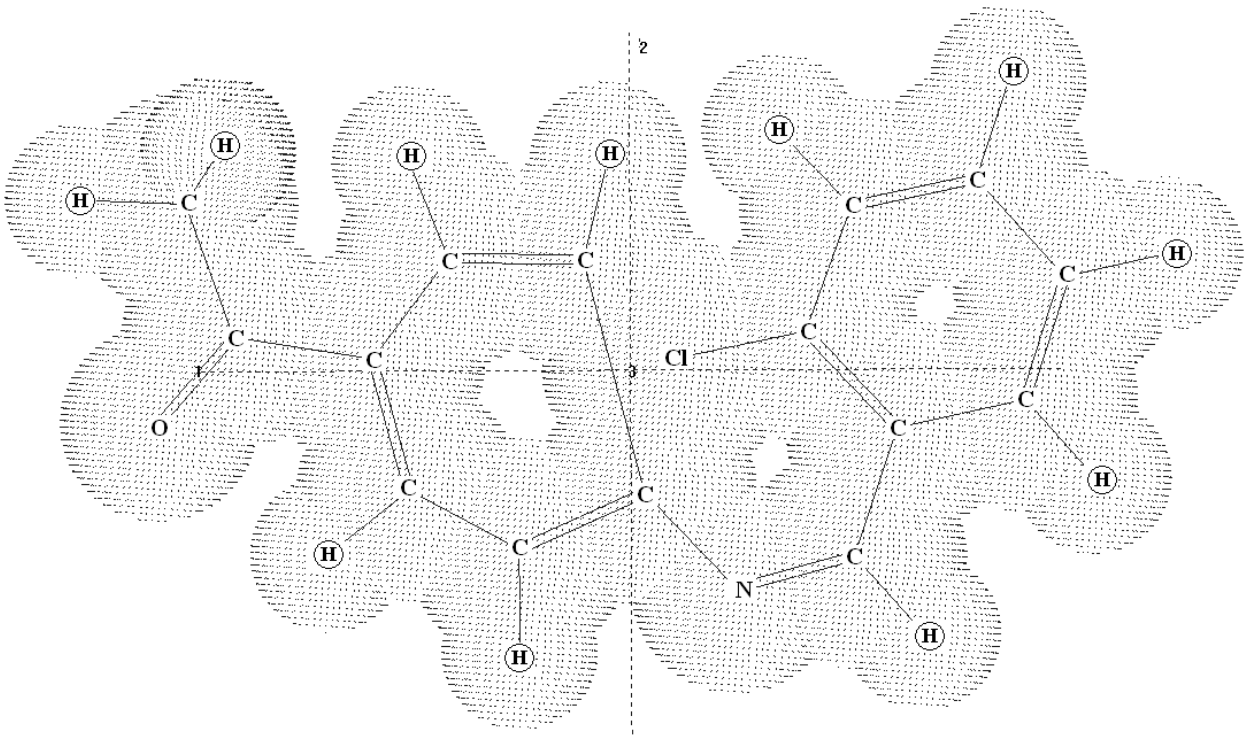

Figure 2. Molecular structure of *N*-(2-chlorobenzylidene)-4-acetylaniline (CBAA) obtained after a geometric optimization procedure using a HyperChem 7.5 software

The CBAA is flat molecule and is stable in air, water and in majority organic solvents. The *N*-(2-chlorobenzylidene)-4-acetylaniline was dissolved at concentrations in the range of 0 - 20 mM in chloride solutions, which were mixed with magnetic stirrer.

2.4. Electrodes and apparatus

The experiments were carried out in a 200 cm^3 glass cell using a three-electrode configuration. The working electrode was prepared from rod of 304 austenic stainless steel in the shape of rectangle which had a surface area of 2 cm^2. Prior to each experiment the working electrode surface was treated with 800, 1200, and 2000 grade emery paper, and then thoroughly rinsed with double distilled water. After this the electrode was degreased with ethanol in an ultrasonic bath (~2 min) and then rinsed with double distilled water. The electrode was then immersed in the test electrolyte.

Electrode potentials were measured and reported against the external saturated calomel electrode (SCE) connected to the cell via a Luggin probe.

A platinum wire was used as an counter electrode. Reference and counter electrodes were individually isolated from the test solution by glass frits.

The polarization measurements were performed using an AutoLab PGSTAT 128N potentiostat.

The values reported in the paper represent mean values of at least three replicate measurements. Moreover, experiments were carried out at suitably well-chosen temperature (± 0.5 ^{0}C) in an air thermostat with the forced air circulation.

2.5. Potentiodynamic experiments

The electrochemical behavior of 304 austenic stainless steel sample in uninhibited and inhibited solution were studied by recording cathodic and anodic potentiodynamic polarization curves. Before polarization scanning, working electrode was immersed in the test electrolyte for 35 min until steady state was attained. The electrode potential was changed in range from -750 to -300 mV vs. SCE at a scan rate of 1 mV s^{-1}. The linear Tafel segments of cathodic and anodic curves were extrapolated to corrosion potential (E_{corr}) to obtain corrosion current densities and the Tafel slopes the cathodic (b_c) and anodic (b_a) were calculated.

The degree of surface coverage (Θ) and the percentage inhibition efficiency (*IE*) were calculated from the following equations [7,13,23]:

$$\Theta = 1 - \frac{j_{corr}}{j^0_{corr}} \quad (1)$$

and:

$$IE(\%) = \frac{j^0_{corr} - j_{corr}}{j^0_{corr}} \times 100 \quad (2)$$

where j^0_{corr} and j_{corr} are the uninhibited and inhibited corrosion current density values, respectively.

2.6. Quantum chemical calculation

HyperChem version 7.5 a quantum–mechanical program from Hypercube Inc (Gainesville, Florida, USA) was used for molecular modeling. The calculation was based on Parametric Method (PM3) *ab* initio semi-empirical method with 3-21G* basis set [13]. Moreover, quantum chemical parameters such as the highest occupied molecular orbital (HOMO), the lowest unoccupied molecular orbital (LUMO), energy gap ($\Delta E = E_{LUMO} - E_{HOMO}$), and dipole moment ($\mu$) were considered.

2.7. Scanning electron microscopy

The surface morphology of the specimens after immersion in 1.2 M Cl^- solution in the absence and presence of 20 mM of *N*-(2-chlorobenzylidene)-4-acetylaniline were tested on a JSM-5400 scanning electron microscope (SEM). The accelerating voltage was 20 kV.

3. RESULTS AND DISCUSSION

3.1. Potentiodynamic measurements

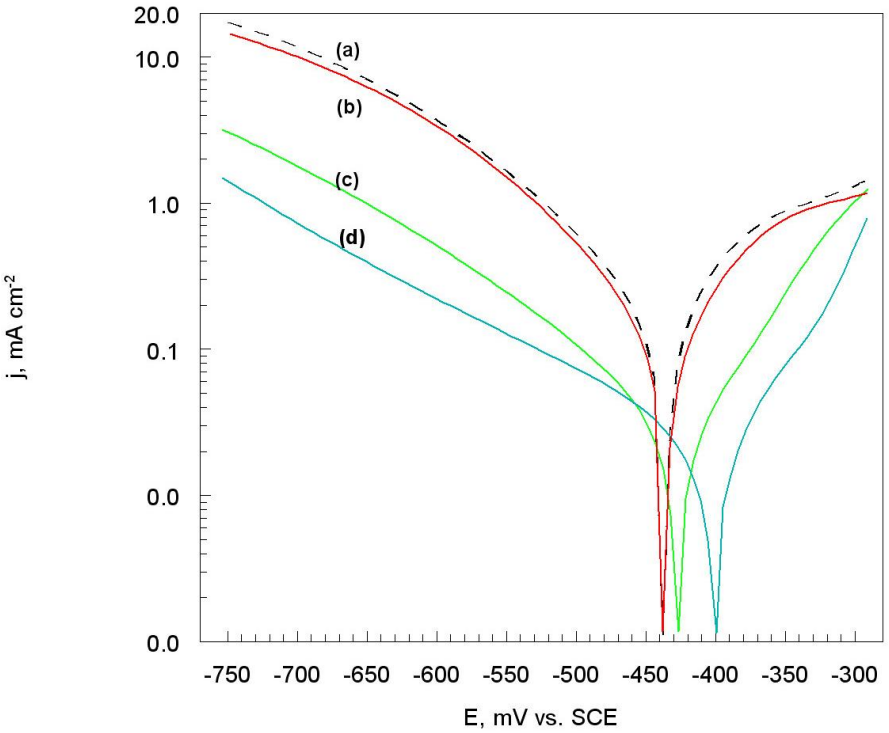

Figure 3. Chosen Tafel plots for 304 austenic stainless steel. Solution containing 1.2 M Cl^- as well as: (a) 0, (b) 1, (c) 10, and (d) 20 mM of *N*-(2-chlorobenzylidene)-4-acetylaniline, dE/dt 1 mV s^{-1}, at temperature 25 ^{0}C

The potentiodynamic behaviour of 304 austenic stainless steel in acid chloride solutions with and without *N*-(2-chlorobenzylidene)-4-acetylaniline at 25 ^{0}C are shown in Figure 3 as Tafel plots.

The cathodic and anodic current density decreases in the presence of the investigated Schiff base. It shows that the addition of CBAA molecules reduces the hydrogen evaluation reaction and also retards the anodic dissolution of ASS.

In chloride acid solution the following corrosion mechanism of austenic stainless steel is proposed [10,25]:

The cathodic hydrogen evaluation:

$$Fe + H^+ = (FeH^+)_{ads} \quad (3)$$
$$(FeH^+)_{ads} \rightarrow (FeH)_{ads} - e^- \quad (4)$$
$$(FeH)_{ads} + H^+ \rightarrow Fe + H_2 - e^-. \quad (5)$$

The anodic dissolution of iron, adsorption tendency of the Cl^- ion onto the ASS surface according to:

$$Fe + Cl^- = (FeCl^-)_{ads} \quad (6)$$
$$(FeCl^-)_{ads} = (FeCl)_{ads} + e^-, \quad (7)$$

which is similar for $(CrCl)_{ads}$ and $(NiCl)_{ads}$. However, at more anodic potential the $(FeCl)_{ads}$ layer dissolves onto the surface electrode, and the local corrosion of steel occur according to the following reactions:

$$(FeCl)_{ads} \rightarrow (FeCl^+) + e^- \quad (8)$$
$$(FeCl^+) = Fe^{2+} + Cl^-, \quad (9)$$

according to similar reaction form ions of Cr^{3+} and Ni^{2+} ions. Moreover, for austenic stainless steel is possible the passivation process. Passivity can be defined as a relatively inactive state in which the metal displays a more noble behaviour than thermodynamic conditions predict [26]. The passivation process followed by the production of a thicker oxide film according to the following sequence:

$$Fe + H^+ + \tfrac{1}{2} O_2 = (FeOH^-)_{ads} \quad (10)$$
$$(FeOH^-)_{ads} = (FeOH)_{ads} + e^- \quad (11)$$
$$(FeOH)_{ads} + H^+ + \tfrac{1}{2} O_2 = Fe(OH)_{2\,(S)} + 3\,e^- \quad (12)$$
$$Fe(OH)_{2\,(S)} + H^+ + \tfrac{1}{2} O_2 \rightarrow FeOOH_{\,(S)} + H_2O + 2\,e^-, \quad (13a)$$

or:

$$2\,FeOOH_{\,(S)} \rightarrow Fe_2O_{3\,(S)} + H_2O. \quad (13b)$$

Moreover, formation of a passive layer can be enriched as a result of following oxides:

$$2\,Cr + 2\,H^+ + 2\,O_2 \rightarrow Cr_2O_{3\,(S)} + H_2O + 14\,e^- \quad (14)$$

$$Ni + 2\,H^{+} + O_2 \rightarrow NiO_{(S)} + H_2O + 6\,e^{-}, \quad (15)$$

(S) concerns to products of reaction which were placed on the surface of electrode.

However, at more anodic potential dissolves the passive layer onto the surface electrode. This means that a passive film on stainless steel is formed even in the acid medium which is a poor electroconductor for which formation and thickening were mainly caused by ionic conductance [27].

The effect of temperature was evaluated by polarization curves test at different temperatures in acid chloride solutions in absence and presence of CBAA, Figure 4. As seen in Figure 4 the cathodic and anodic current density increases with an increase in the temperature of solution.

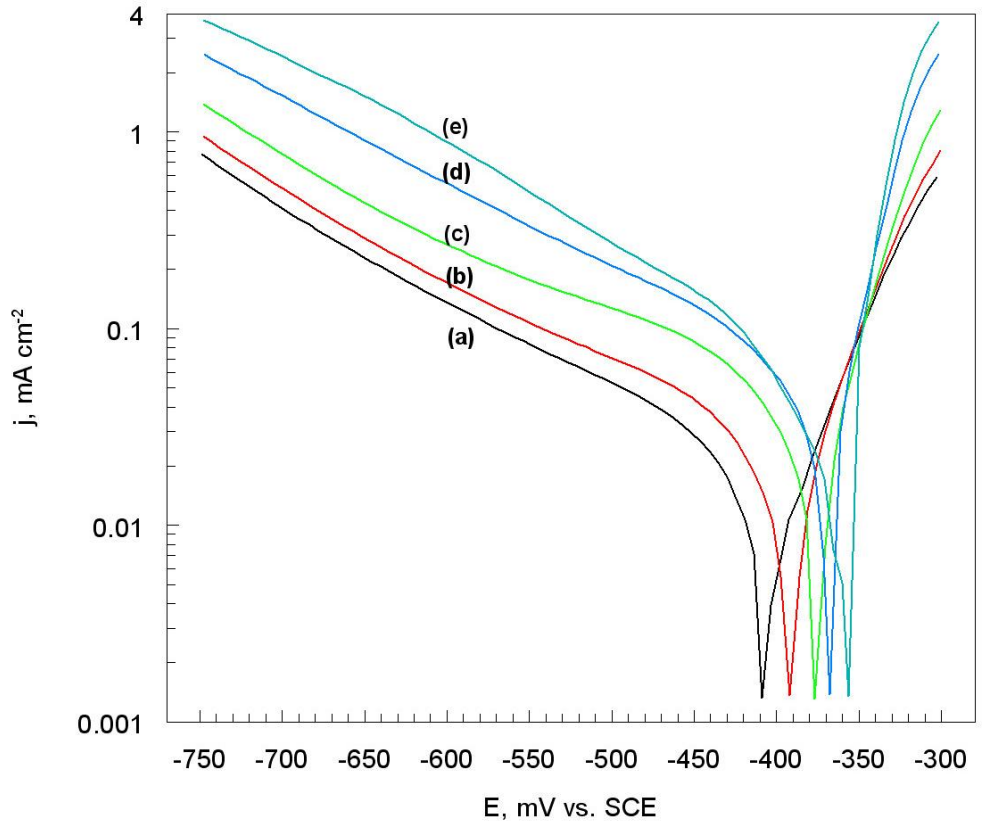

Figure 4. Tafel plots for 304 austenic stainless steel. Solution containing 1.2 M Cl^{-} and 20 mM of *N*-(2-chlorobenzylidene)-4-acetylaniline, at temperatures: (a) 25, (b) 30, (c) 40, (d) 50, and (e) 60 ^{0}C, dE/dt 1 mV s^{-1}

Corrosion parameters i.e. corrosion potential (E_{corr}), cathodic and anodic Tafel slopes (b_c) and (b_a), and corrosion current density (j_{corr})) obtained from the Tafel extrapolation method of the polarization curves are given in Table 1. It should be noted that E_{corr} shifted towards more positive values with an increase in the temperature and concentration of CBAA.A compound can be classified as a cathodic or an anodic type inhibitor when the change in the E_{corr} values is larger than ±85 mV with respect to the corrosion potential of the blank [28].

Table 1. Corrosion parameters for 304 austenic stainless steel in a 1.2 M Cl^- in the absence and presence of *N*-(2-chlorobenzylidene)-4-acetylaniline, and corresponding degree of surface coverage at different temperatures

Temperature ^0C	Concentration mM	E_{corr} mV	$-b_c$ mV dec^{-1}	b_a mV dec^{-1}	j_{corr} mA cm^{-2}	Θ
25	Blank	-442	50	35	0.240	------
	1	-438	55	30	0.130	0.458
	5	-430	57	28	0.074	0.691
	10	-425	60	25	0.028	0.883
	15	-414	68	23	0.025	0.896
	20	-408	70	20	0.022	0.908
30	Blank	-437	50	40	0.370	------
	1	-430	60	40	0.190	0.486
	5	-423	58	26	0.110	0.703
	10	-417	55	20	0.038	0.897
	15	-399	69	18	0.031	0.916
	20	-392	75	15	0.025	0.932
40	Blank	-410	60	55	0.800	------
	1	-420	60	40	0.220	0.725
	5	-412	62	20	0.130	0.838
	10	-402	65	15	0.048	0.940
	15	-384	75	14	0.045	0.944
	20	-375	80	15	0.042	0.948
50	Blank	-399	65	95	1.780	------
	1	-395	65	30	0.340	0.809
	5	-388	59	18	0.200	0.888
	10	-381	60	10	0.068	0.962
	15	-376	65	14	0.060	0.966
	20	-368	70	13	0.058	0.967
60	Blank	-395	75	120	2.780	------
	1	-375	65	30	0.490	0.824
	5	-370	60	14	0.290	0.896
	10	-365	58	5	0.083	0.970
	15	-360	60	6	0.078	0.972
	20	-355	62	8	0.074	0.973

Since the largest displacement exhibited by CBAA were about 40 mV at different temperature of solutions (Table 1). It may be concluded that of *N*-(2-chlorobenzylidene)-4-acetylaniline in acid chloride environment should be considered as a mixed-type inhibitor. Moreover, the cathodic (b_c) and anodic (b_a) Tafel slopes (Table 1) of CBAA were found to change with temperatures and inhibitor concentration, this indicates that of *N*-(2-chlorobenzylidene)-4-acetylaniline affected both of these reactions [29]. Results presented in Table 1 show that an increase in temperature increases the corrosion current density, while the addition of CBAA decreases the j_{corr} values as compared to the control (blank) values across the temperature range indicates the inhibiting effect of Schiff base.

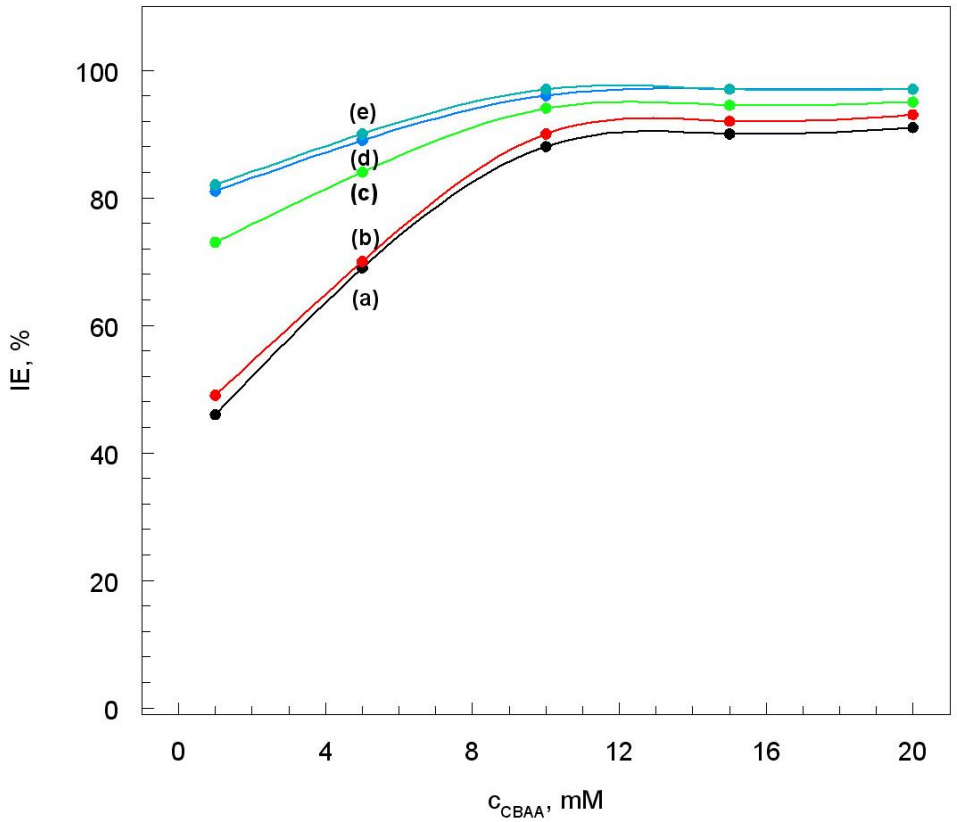

Figure 5. Corrosion inhibition efficiency for 304 austenic stainless steel in a 1.2 M Cl^- solution in the presence of *N*-(2-chlorobenzylidene)-4-acetylaniline, at temperatures: (a) 25, (b) 30, (c) 40, (d) 50, and (e) 60 ^{0}C

The degree of surface coverage was calculated from the Equation (1). The results (Table 1) showed that the Θ increased with in temperature and the concentration of *N*-(2-chlorobenzylidene)-4-acetylaniline. Consequently, the corrosion inhibition efficiency can also be calculated from polarization tests by using the Equation (2) the values *IE* are presented in Figure 5. The inhibition efficiency increases with an increase both concentration (especially for small concentration) of inhibitor, and temperature of the solution. Such behaviour of *N*-(2-chlorobenzylidene)-4-acetylaniline proves about strong adsorption of CBAA onto the 304 austenic stainless steel surface. Adsorption is the mechanism generally accepted to explain the inhibitory action of organic corrosion inhibitors.

The adsorption of inhibitors can affect the corrosion process in two ways: (i) by decreasing the available reaction area (geometric blocking effect), and (ii) by modifying the activation energy of the cathodic and/or anodic reactions [30]. This problem will be discussed in the next part of the work.

3.2. Activation parameters

Thermodynamic activation parameters have an important role in understanding the inhibitive mechanism of organic inhibitors. Activation parameters such as: the activation of energies (E_a), the enthalpy of activation (ΔH_a), and the entropy of activation (ΔS_a) were calculated from an Arrhenius-type plot [30,31]:

$$j_{corr} = A \exp\left(\frac{-E_a}{RT}\right) \quad (16)$$

and transition-state:

$$j_{corr} = \left(\frac{RT}{N\,h}\right) \exp\left(\frac{\Delta S_a}{R}\right) \exp\left(\frac{-\Delta H_a}{RT}\right) \quad (17)$$

where A is the Arrhenius constant, N is the Avogadro's constant, h is the Planck's constant, R is the universal gas constant, and T is the absolute temperature.

Plots of ln (j_{corr}) vs. 1 / T, Figure 6, and ln (j_{corr} / T) vs. 1 / T, Figure 7 give straight lines with slopes of $-E_a / R$, and $-\Delta H_a / R$ respectively.

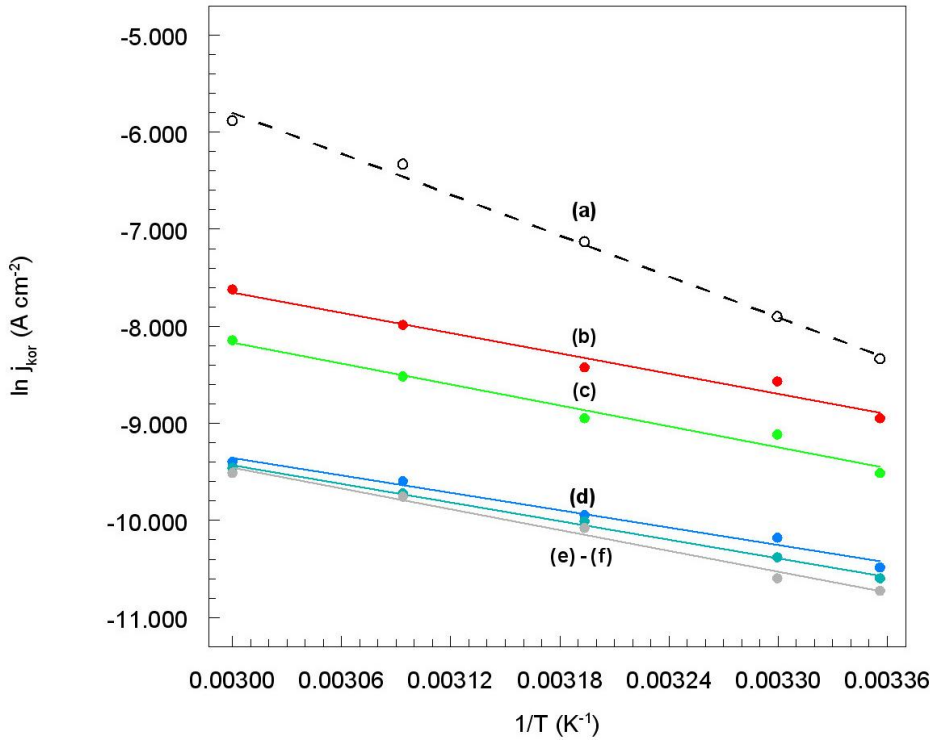

Figure 6. Arrhenius plots for 304 austenic stainless steel. Solution containing 1.2 M Cl^- as well as: (a) 0, (b) 1, (c) 5, (d) 10, (e) 15, and (f) 20 mM of *N*-(2-chlorobenzylidene)-4-acetylaniline

Corrosion kinetic parameters for the ASS obtained from these graphs are given in Table 2. The value the energy of activation was higher for uninhibited solution (59 kJ mol^{-1}), than in presence of Schiff base (29 kJ mol^{-1}). The lower activation energy in the presence of inhibitor is indication for its chemisorption [13].

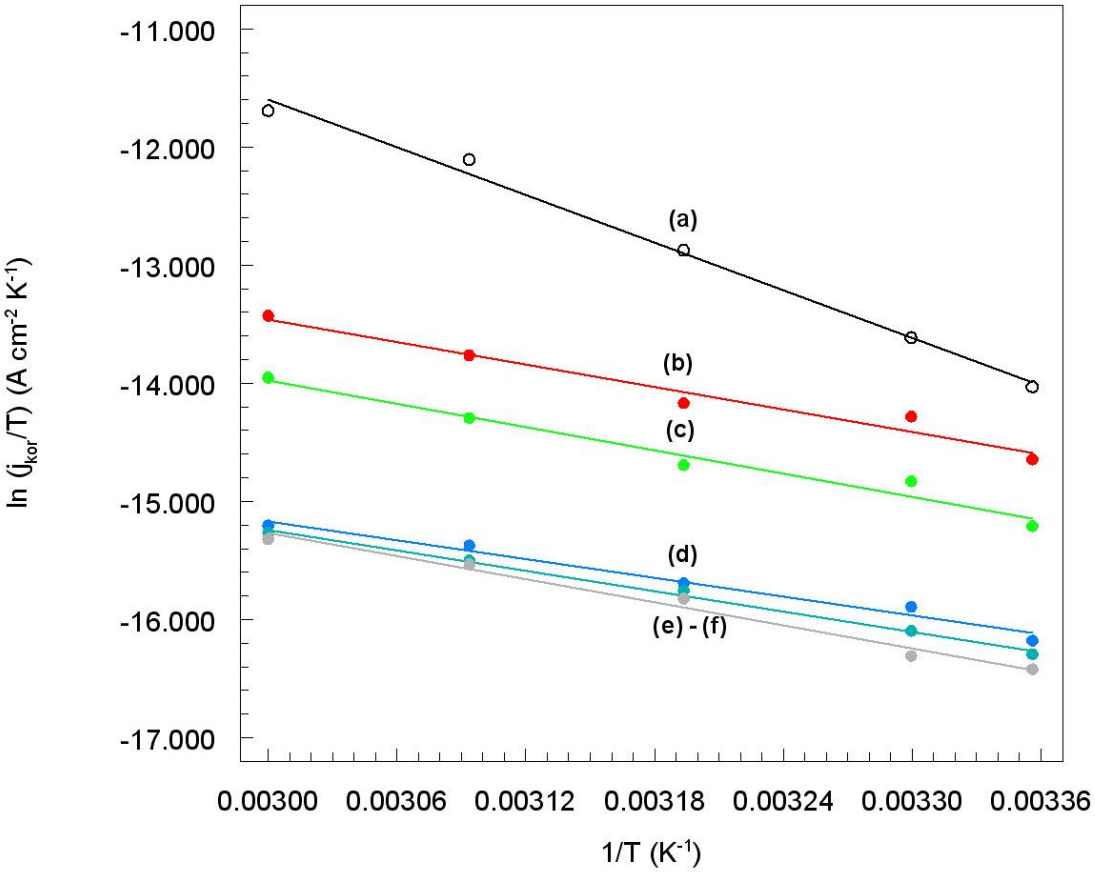

Figure 7. Transition state plots for 304 austenic stainless steel. Solution containing 1.2 M Cl^- as well as: (a) 0, (b) 1, (c) 5, (d) 10, (e) 15, and (f) 20 mM of *N*-(2-chlorobenzylidene)-4-acetylaniline

After addition to corrosive solution 20 mM of *N*-(2-chlorobenzylidene)-4-acetylaniline the energies of activation diminishes about twice only (Table 2). However, E_a does not change significantly which is characteristic for mixed type (physical and chemical) adsorption of CBAA onto the ASS surface. The positive signs the enthalpy of activation, ΔH_a reflect the endothermic process, which is attributable unequivocally to chemisorption. Moreover, the enthalpy of chemisorption process approaches 100 kJ mol^{-1} [32-34]. In the present study the ΔH_a value for 20 mM of CBAA was found 27 kJ mol^{-1} (Table 2) indicated that it is adsorbed onto the 304 austenic stainless steel surface by both physical and chemical process.

The values of entropy activation, ΔS_a for different concentration of CBAA are listed in Table 2.

Table 2. Corrosion kinetic parameters for 304 austenic stainless steel in a 1.2 M Cl^- in the absence and presence of different concentrations of *N*-(2-chlorobenzylidene)-4-acetylaniline

Concentration mM	E_a kJ mol^{-1}	ΔH_a kJ mol^{-1}	ΔS_a J mol^{-1} K^{-1}
Blank	59.05	56.43	-124.51
1	29.29	26.68	-229.32
5	30.11	27.49	-231.21
10	24.92	22.30	-256.67
15	26.74	24.12	-251.83
20	29.95	27.32	-242.45

The large and negative values of ΔS_a imply that the activated complex in the rate determining step represents an association rather than a dissociation step, meaning that a decrease in disordering takes place on going from reactants to the activated complex.

3.3. Adsorption parameters

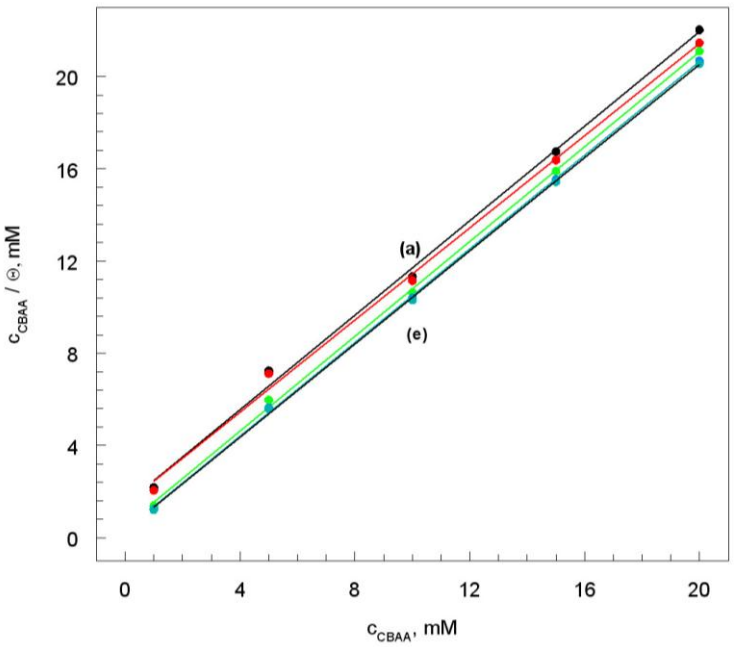

Figure 8. Adsorption isotherms of *N*-(2-chlorobenzylidene)-4-acetylaniline on the 304 austenic stainless steel in a 1.2 M Cl^- solution at different temperatures; (a) 25, (b) 30, (c) 40, (d) 50, and (e) 60 ^{0}C

The efficiency of organic molecules as good corrosion inhibitors mainly depends on their adsorption ability onto the metal surface. The inhibition efficiency is a function of the electrode surface covered by the inhibitor molecules. The degree of surface coverage for the *N*-(2-chlorobenzylidene)-4-acetylaniline at different temperatures were depicted in Table 1. The adsorption isotherms can provide important clues to the nature of metal-inhibitor interaction it was established isotherms that describe the adsorptive behaviour of the inhibitor.

It was assumed that the adsorption of *N*-(2-chlorobenzylidene)-4-acetylaniline onto the ASS surface was described by the Langmuir isotherm [17,30,33].

The plot of $c_{\mathrm{CBAA}} / \Theta$ vs. c_{CBAA} yields a straight lines, Figure 8 supporting the assumption that the adsorption of CBAA from chloride acid solution onto the ASS surface at the studied temperatures obeys a Langmuir adsorption isotherm which is represented by:

$$\frac{c_{CBAA}}{\Theta} = \frac{1}{K_{ads}} + c_{CBAA} \quad (18)$$

where c_{CBAA} is the inhibitor concentration, K_{ads} is the equilibrium constant for the adsorption/desorption process.

From the intercepts of the straight lines on the c_{CBAA} / 0 axis one can calculated, K_{ads} values that relate the standard free energy of adsorption by:

$$\Delta G^0_{ads} = -RT\,ln\left(55.5 \times K_{ads}\right) \quad (19)$$

where the constant 55.5 is the molar concentration of water in solution. The thermodynamic parameters for adsorption process obtained from Langmuir adsorption isotherms for the studied inhibitor are given in Table 3.

The absolute standard free energy of the adsorption values increase with temperature. The negative values of ΔG^0_{ads} indicate spontaneous adsorption of *N*-(2-chlorobenzylidene)-4-acetylaniline on the steel surface. The values of ΔG^0_{ads} were changed in range from -26 to -29 kJ mol^{-1} it is suggested that adsorption of Schiff base involves the physical and chemical adsorption of inhibitor onto the ASS surface in chloride acid solution at the studied temperatures.

Thermodynamically (ΔG^0_{ads}) is related to the standard enthalpy (ΔH^0_{ads}) and entropy (ΔS^0_{ads}) of the adsorption process according equation:

$$\Delta G^0_{ads} = \Delta H^0_{ads} - T\,\Delta S^0_{ads} \quad (20)$$

The standard enthalpy of adsorption can be calculated according to the Van't Hoff equation:

$$ln\,K_{ads} = \frac{-\Delta H^0_{ads}}{RT} + const \quad (21)$$

A plot of *ln* K_{ads} vs. 1 / *T* gives straight line, as shown in Figure 9. The slope of the straight line is $-\Delta H^0_{ads}/R$. The value of standard free enthalpy of the adsorption is given in Table 3. Since the ΔH^0_{ads} is positive this means that the adsorption of *N*-(2-chlorobenzylidene)-4-acetylaniline molecules onto the 304 austenic stainless steel surface is an endothermic process, which is attributable unequivocally to chemisorptions [32-34].

Table 3. Slope of adsorption isotherm, linear correlation coefficient, equilibrium constant adsorption/desorption and standard free: energy, enthalpy, and entropy of the adsorption for 304 austenic stainless steel in a 1.2 M Cl^- solution in the presence of *N*-(2-chlorobenzylidene)-4-acetylaniline at different temperatures

Temperature ^{0}C	*b*	*R*	$K_{ads} \times 10^3$ M^{-1}	$-\Delta G^\circ_{ads}$ kJ mol^{-1}	ΔH°_{ads} kJ mol^{-1}	ΔS°_{ads} J mol^{-1} K^{-1}
25	1.02	0.9986	6.84×10^2	26.15		228.99
30	1.00	0.9985	6.98×10^2	26.18		229.09
40	1.02	0.9997	1.95×10^3	28.72	42.09	237.62
50	1.01	0.9998	3.02×10^3	29.80		241.24
60	1.01	0.998	3.24×10^3	29.98		241.84

The values of standard free entropy of the adsorption are depicted in Table 3. The signs of ΔS^0_{ads} are positive, values in the presence of inhibitor are large, and increased as compared to free acid solution. The adsorption of CBAA from the aqueous solution can be regarded as substitution process between the inhibitor in the aqueous phase and water molecules onto the ASS surface [35,36]:

$$CBAA_{(sol)} + H_2O_{(ads)} \leftrightarrow CBAA_{(ads)} + H_2O_{(sol)}, \quad (22)$$

at present it is known that one adsorbed H_2O molecule is replaced by one of *N*-(2-chlorobenzylidene)-4-acetylaniline molecule onto the 304 austenic stainless steel surface. The substitution adsorption process may be exothermic, and the increase in entropy becomes the driving force for the adsorption of CBAA onto the ASS surface. The thermodynamic values obtained are the algebraic sum of adsorption of organic inhibitor molecule and desorption of water molecule.

3.4. Quantum chemical study

It is well known that molecular structure of the inhibitor plays a vital role in determining its mode of adsorption onto the corroded surface. To investigate the correlation between molecular

structure of *N*-(2-chlorobenzylidene)-4-acetylaniline and its inhibition effect, quantum chemical parameters has been performed.

Protection efficiency of inhibitors depends on the electronic properties of the corrosion inhibitors such as: highest occupied molecular orbital (HOMO), the lowest unoccupied molecular orbital (LUMO). It has been reported [37-39] that the higher the HOMO energy of the inhibitor the greater the trend of offering electrons to unoccupied *d* orbital of the metal, and the higher the corrosion efficiency. In addition, the lower the LUMO energy the easier the acceptance of electrons from metal surface [40,41]. The frontier molecular orbital density distributions of HOMO and LUMO for CBAA were shown in Figure 10.

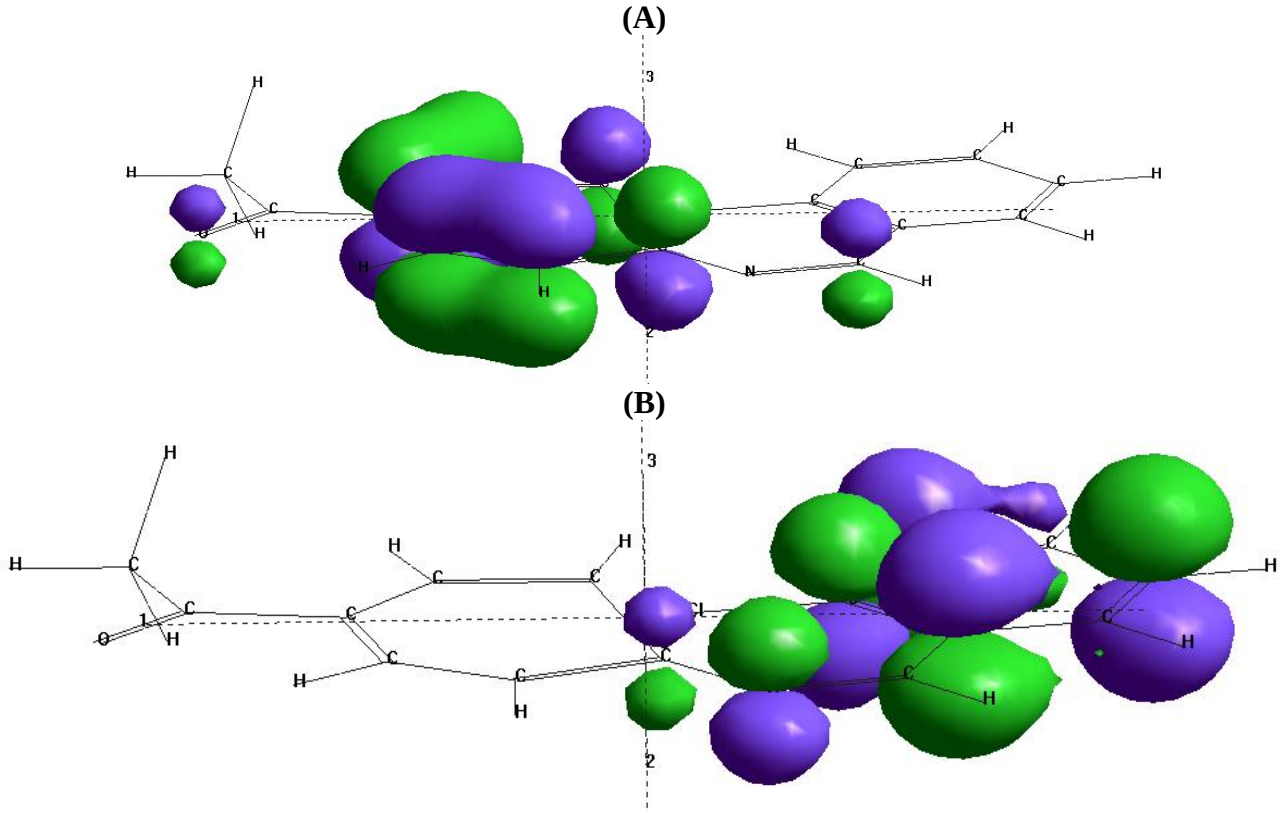

Figure 10. The frontier molecular orbital density distribution for *N*-(2-chlorobenzylidene)-4-acetylaniline: (A) HOMO, (B) LUMO

Table 4. The calculated quantum chemical parameters for *N*-(2-chlorobenzylidene)-4-acetylaniline

Inhibitor	E_{HOMO}	E_{LUMO}	ΔE	μ	I	A	χ	η	ΔN
	eV	eV	eV	D	eV	eV	eV	eV	
CBAA	-8.556	-2.244	6.312	9.393	8.556	2.244	5.400	3.156	0.253

The calculated quantum chemical parameters for *N*-(2-chlorobenzylidene)-4-acetylaniline were listed in Table 4. The higher value of E_{HOMO} suggests that the CBAA molecule offering electrons to

unoccupied *d* orbital of the metal atom creating strong bond between surface of ASS and CBAA molecules.

Attentively observing to the Figure 10 it is understandable that *N*-(2-chlorobenzylidene)-4-acetylaniline also could accept the *d*-orbital electrons of iron by LUMO on the benzene ring. Consequently, this electron acceptance could help to form more stable bond between inhibitor molecule and iron surface. Moreover, the results obtained show that of CBAA has the low value of energy gap and the high value of dipole moment (Table 4) which will favor the enhancement of corrosion inhibition by the adsorption of *N*-(2-chlorobenzylidene)-4-acetylaniline onto the ASS surface.

The energies of the HOMO and the LUMO orbitals of the inhibitor molecule are related to the ionization potential, $I = -E_{HOMO}$, and electron affinity, $A = -E_{LUMO}$ of the studied molecule [39-42], are placed in Table 4. The values of I and A were considered for the calculation of the electronegativity (χ) and the global hardness (η) using the following relations:

$$\chi = \frac{I + A}{2} \quad (23)$$

and:

$$\eta = \frac{I - A}{2} \quad (24)$$

The calculated parameters are listed in Table 4.

The number of transferred electrons (ΔN) from the inhibitor molecule to the iron atom was calculated according to formula [39-42]:

$$\Delta N = \frac{\chi_{Fe} - \chi_{inh}}{2(\eta_{Fe} + \eta_{inh})} \quad (25)$$

where χ_{Fe} and χ_{inh} denote the absolute electronegativity of iron and the molecule, respectively.

The idea behind this is that in the reaction of two systems with different electronegativity as a metallic surface and an inhibitor molecule the following mechanism will take place: the electron flow will move from the molecule with the low electronegativity towards that of a higher value until the chemical potentials are the same.

The theoretical values of χ_{Fe} and η_{Fe} are 7.0 and 0 eV mol^{-1}, respectively [42-44]. The fraction of electrons transferred from *N*-(2-chlorobenzylidene)-4-acetylaniline to the metal molecule was calculated (Table 4). The value of ΔN showed inhibition effect of CBAA resulted from electron donation. However, the *N*-(2-chlorobenzylidene)-4-acetylaniline was the donators of electrons while the ASS was acceptor. However, *N*, *O*, and *Cl* (Fig. 2) have the most probability to form coordinating bond. The CBAA was bound onto the 304 surface and thus formed inhibition adsorption layer against corrosion.

3.5. Scanning electron microscopy studies

The surface morphology of stainless steel samples immersed in 1.2 M Cl^- solution for 24 hours in the absence and in the presence of *N*-(2-chlorobenzylidene)-4-acetylaniline were studied by scanning electron microscopy. The solutions were not degassed.

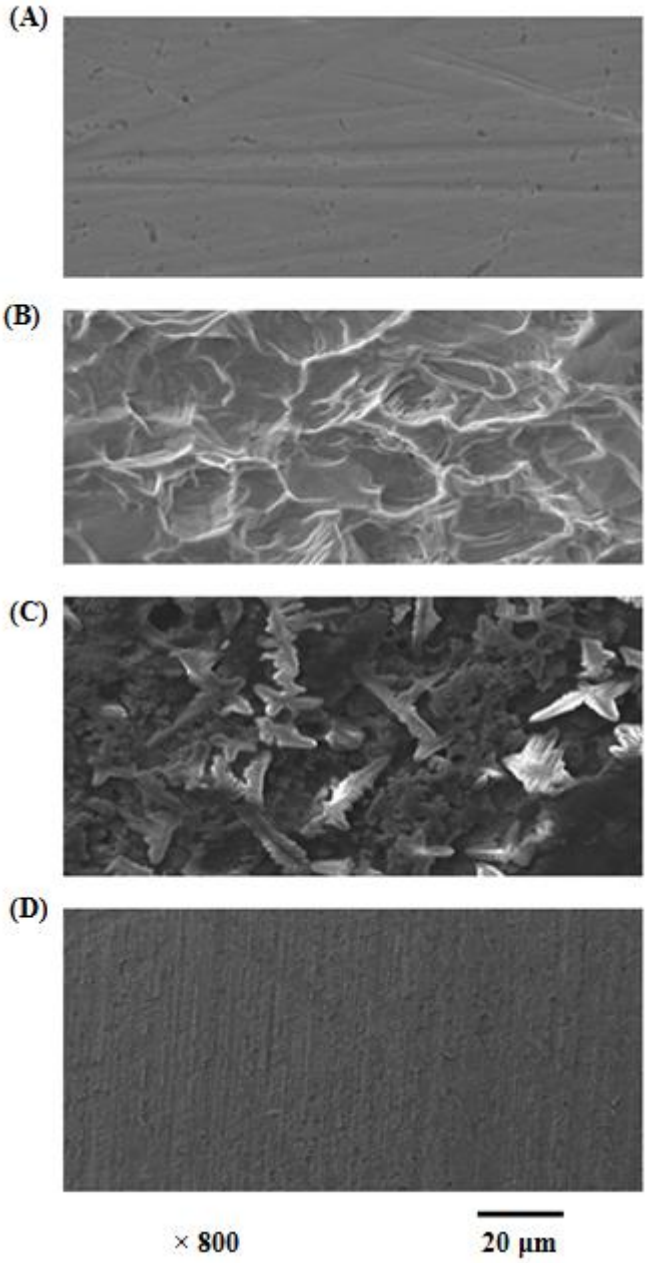

Figure 11. SEM micrographs of 304 austenic stainless steel surface: (A) before immersion to solution of chlorides, (B) and (C) after exposition (24 hours) in a 1.2 M Cl^- solution or in the presence 20 mM of *N*-(2-chlorobenzylidene)-4-acetylaniline respectively, (D) after removal of the inhibiting film

Figure 11 show the surface morphology of 304 austenic stainless steel specimens (A) before and (B) after being immersed in corrosive solution. The photograph 11 (B) revels that the surface was

strongly damaged in absence of the inhibitor. Figure 11 (C) show SEM image of ASS surface after immersion (for the same time interval) in corrosive solution containing additionally 20 mM of CBAA. The SEM photograph show that protective layer appears onto the surface of steel. The inhibitor film does not cover tightly the surface, and hence does not protect austenic stainless steel surface to an adequate degree. The Figure 11 (D) presents sample after the removal of the inhibiting film. Chloride ions, oxygen and water penetrate the protective film through pores, flaws or other weak spots what results in the further corrosion of 304 austenic stainless steel.

4. MECHANISM OF INHIBITION

The corrosion inhibition mechanism in acid medium the most often depends on the adsorption of an inhibitor onto the metal surface. The inhibitive action of inhibitors depends on the electron densities around the adsorption centers. The higher the electron density at the centre, the more efficient is the inhibitor.

The adsorption of the inhibitor onto metal surface is the first step in the action mechanism of inhibition. Physical adsorption requires presence of both electrically charged surface of the metal and charged species in the bulk of the solution. Moreover, chemical adsorption requires in the presence of a metal to have a vacant low-energy electron orbital, and an inhibitor with molecules having relatively loosely bond electrons or heteroatom with lone pair electrons.

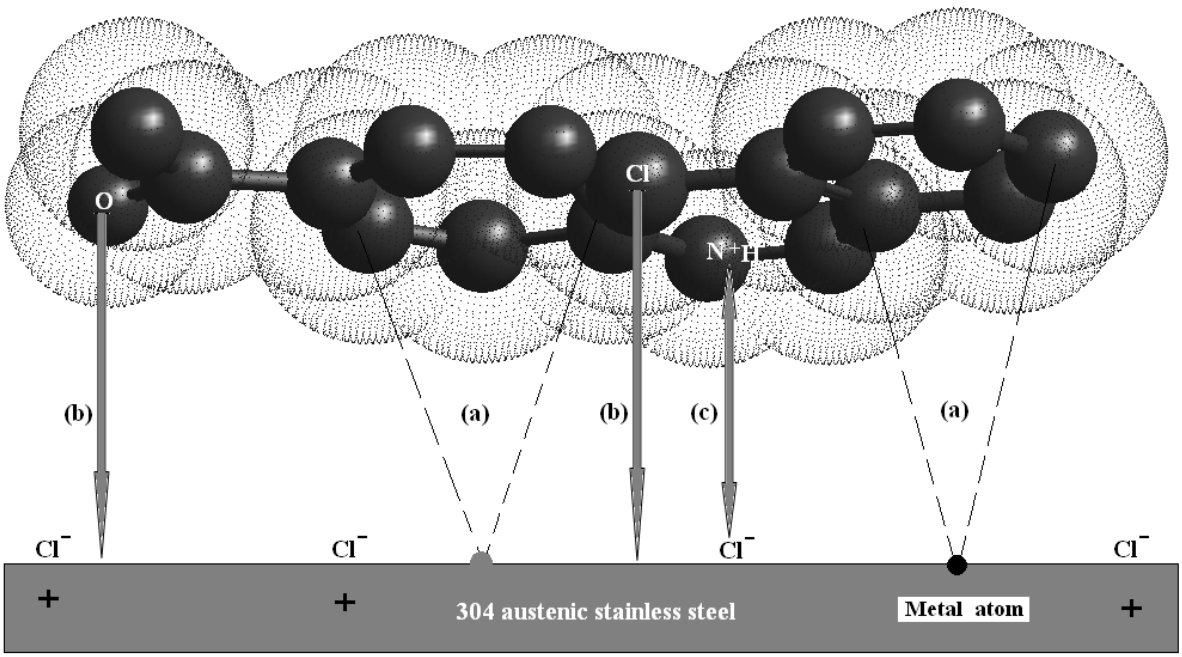

Figure 12. Proposal of model of protective layer of *N*-(2-chlorobenzylidene)-4-acetylaniline on 304 austenic stainless steel surface in a 1.2 M Cl^- solution: (a) chemisorptions, (b) feedback bond, and (c) electrostatic interaction (physisorption)

The studied of *N*-(2-chlorobenzylidene)-4-acetylaniline as an inhibitor is organic base (Schiff base) which contains of an imine group (─CH=N─) (Fig. 2). The imine group determines propriety of this kind of compounds. The addition of acid or a base to the aqueous solution of any of these inhibitor will transform the neutral molecule into a cation or an anion. In aqueous acid solution the CBAA molecule was protonated according to the reaction:

$$CBAA + H^+ \leftrightarrow CBAAH^+, \quad (26)$$

thus they become cation, existing in equilibrium with the corresponding molecular form. The molecular and cation both forms played separate role in the adsorption of inhibitor onto the metal surface.

The protective layer has been formed according to:

$$(Fe - Cl)_{ads} + CBAAH^+ \leftrightarrow (Fe - CBAA)_{ads} + H^+ + Cl^-, \quad (27)$$

according to similar reaction form compounds of $(Cr–CBAA)_{ads}$, and $(Ni–CBAA)_{ads}$. The inhibiting effect of *N*-(2-chlorobenzylidene)-4-acetylaniline can be regarded as an adsorption of inhibitor and the formation compound protective film onto steel surface, whose proposal of model is presented in Figure 12. Therefore, it may be assumed that of CBAA adsorption can also occur via electrostatic interaction (physisorption) with the surface of the electrode.

The adsorption of *N*-(2-chlorobenzylidene)-4-acetylaniline onto the ASS surface makes a barrier for mass and charge transfers. This situation leads to the protection of austenic stainless steel surface from the attack of aggressive anions, Cl^- of the solution.

5. CONCLUSION

The inhibition effect of *N*-(2-chlorobenzylidene)-4-acetylaniline on the corrosion of 304 austenic stainless steel in chloride acid solutions was studied. From the data obtained the following points can be emphasized:

(1) The corrosion of 304 austenic stainless steel in a 1.2 M Cl^- solution is significantly reduced by addition of *N*-(2-chlorobenzylidene)-4-acetylaniline.

(2) The CBAA behaves as mixed type corrosion inhibitor.

(3) Langmuir adsorption isotherm exhibited the best fit to the experimental data.

(4) The inhibition efficiency corrosion of ASS increases with increase of concentration of *N*-(2-chlorobenzylidene)-4-acetylaniline, and in increase of temperature of solution.

(5) Thermodynamic activation parameters reflect the endothermic nature dissolution process of 304 austenic stainless steel.

(6) Thermodynamic adsorption parameters show that of *N*-(2-chlorobenzylidene)-4-acetylaniline was adsorbed by spontaneous, endothermic process which is unequivocally to chemical adsorption of inhibitor.

(7) Quantum chemical method shows that of CBAA molecule can be directly adsorbed at the steel surface on the basis of donor-acceptor interactions between the π-electrons of benzene ring, and *N, O, and Cl* atoms, or the vacant *d*-orbital of metal atoms.

(8) SEM micrographs showed that the *N*-(2-chlorobenzylidene)-4-acetylaniline molecules form a protective film onto the ASS surface.

ACKNOWLEDGMENTS
This work was supported by the ESF Human Capital Operational Programme grant 6/1/8.2.1./POKL/ 2009.

References

1. C-O. A. Olsson, D. Landolt, *Electrochim. Acta* 48 (2003) 1093.
2. M. Da Cunha Belo, M. Walls, N.E. Hakiki, J. Corset, E. Picquenard, G. Sagon, D. Noël, *Corros. Sci.* 40 (1998) 447.
3. A. Yağan, N.Ö. Permez, A. Yıldız, *Corros. Sci.* 49 (2007) 2905.
4. S. Şafak, B. Duran, A. Yurt, G. Türkoğlu, *Corros. Sci.* 54 (2012) 251.
5. K. Emregül, O. Atakol, *Mater. Chem. Phys.* 83 (2004) 373.
6. U. Aytaç, Ü. Özmen, M. Kabasakaloğlü, *Mater. Chem. Phys.* 89 (2005) 176.
7. M. Behpour, S.M. Ghoreishi, M. Salavati-Niasari, B. Ebrahimi, *Mater. Chem. Phys.* 107 (2008) 153.
8. N. Soltani, M. Behpour, S.M. Ghoreishi, H. Naeimi, *Corros. Sci.* 52 (2010) 1351.
9. M.G. Hosseini, S.F.L. Mertens, M. Ghorbani, M.R. Arshadi, *Mater. Chem. Phys.* 78 (2003) 800.
10. A. Yurt, A. Balaban, S.U. Kandemir, G. Bereket, B. Erk, *Mater. Chem. Phys.* 85 (2004) 420.
11. M. Lashgari, M.R. Arshdi, S. Miandari, *Electrochim. Acta* 55 (2010) 6058.
12. Y.K. Agrawal, J.D. Talati, M.D. Shah, M.N. Desai, N.K. Shah, *Corros. Sci.* 46 (2004) 633.
13. M. Behpour, S.M. Ghoreishi, N. Mohammadi, M. Salavati-Niasari, *Corros. Sci.* 53 (2011) 3380.
14. M. Behpour, S.M. Ghoreishi, N. Soltani, M. Salavati-Niasari, *Corros. Sci.* 51 (2009) 1073.
15. C. Küstü, K.C. Emregül, O. Atakol, *Corros. Sci.* 49 (2007) 2800.
16. H.D. Leçe, K.C. Emregül, O. Atakol, *Corros. Sci.* 50 (2008) 1460.
17. M.G. Hosseini, M. Ehteshamzadeh, T. Shahrabi, *Electrochim. Acta* 52 (2007) 3680.
18. R.A. Prabhu, T.V. Venkatesha, A.V. Shanbhag, G.M. Kulkarni, R.G. Kalkhambkar, *Corros. Sci.* 50 (2008) 3356.
19. K.S. Jacob, G. Parameswaran, *Corros. Sci.* 52 (2010) 224.
20. I. Ahamad, R. Prasad, M.A. Quraishi, *Mater. Chem. Phys.* 124 (2010) 1155.
21. M.A. Hegazy, M.F. Zaky, *Corros. Sci.* 52 (2010) 1333.
22. P.C. Okafor, Y. Zheng, *Corros. Sci.* 51 (2009) 850.
23. I.B. Obot, N.O. Obi-Egbedi, S.A. Umoren, *Corros. Sci.* 51 (2009) 1868.
24. Z. Begum, A. Poonguzhali, R. Basu, C. Sudha, H. Shaikh, R.V. Subba Rao, *Corros. Sci.* 53 (2011) 1424.
25. I.O.M. Bockris, B. Young, *J. Electrochem. Soc.* 139 (1991) 2237.
26. N.E. Hakiki, *Corros. Sci.* 53 (2011) 2688.
27. M.S.S. Morad, A.A.A. Hermas, *J. Chem. Technol. Biotechnol.* 76 (2001) 401.
28. W. Li, Q. He, S. Zhang, C. Pei, B. Hou, *J. Appl. Electrochem.* 38 (2008) 289.
29. F.G. Liu, M. Du, J. Zhang, M. Qiu, *Corros. Sci.* 51 (2009) 102.
30. A.Y. Musa, A.A.H. Kadhum, A.B. Mohamad, M.S. Takriff, A.R. Daud, S.K. Kamarudin, *Corros. Sci.* 52 (2010) 526.

31. A.Y. Musa, A.A.H. Kadhum, A.B. Mohamad, M.S. Takriff, *Mater. Chem. Phys.* 129 (2011) 660.
32. S. Martinez, I. Stern, *Appl. Surf. Sci.* 199 (2002) 83.
33. A.K. Singh, M.A. Quraishi, *Corros. Sci.* 51 (2009) 2752.
34. A.K. Singh, M.A. Quraishi, *Corros. Sci.* 52 (2010) 152.
35. M. Şahin, S. Bilgiç, H. Yılmaz, *Appl. Surf. Sci.* 195 (2002) 1.
36. J. Trela, M. Scendo, *Corrosion Protection* 55 (2012) 86.
37. S. Ramachandran, B.L. Tsai, M. Blanco, H. Chen, Y. Tang, W.A. Goddard, *J. Phys. Chem.* A 101 (1997) 83.
38. I. Lukovits, K. Palfi, E. Kalman, *Corrosion* 53 (1997) 915.
39. E.H. El-Ashri, A. El-Nemr, S.A. Essawy, S. Ragub, *Electrochim. Acta* 51 (2006) 3957.
40. N.O. Obi-Egbedi, I.B. Obot, *Corros. Sci.* 53 (2011) 263
41. S.E. Nataraja, T.V. Venkatesha, K. Manjunatha, B. Poojary, M.K. Pavithra, H.C. Tandon, *Corros. Sci.* 53 (2011) 2651.
42. H. Ju, Z. Kai, Y. Li, *Corros. Sci.* 50 (2008) 865.
43. A.Y. Musa, A.A.H. Kadhum, A.B. Mohamad, A.A.B. Rahoma, H. Mesmari, *J. Mol. Struct.* 969 (2010) 233.
44. M. Scendo, J. Trela, N. Radek, *Corros. Rev.* 30 (2012) 33.